

On the cosmic ray bound for models of extragalactic neutrino production

Karl Mannheim

Universitäts-Sternwarte, Geismarlandstr. 11, D-37083 Göttingen, Germany; kmannhe@uni-sw.gwdg.de

R.J. Protheroe

Department of Physics and Mathematical Physics, The University of Adelaide, Adelaide, Australia 5005; rprother@physics.adelaide.edu.au

Jörg P. Rachen

Sterrenkundig Instituut, Universiteit Utrecht, NL-3508 TA Utrecht, The Netherlands; J.P.Rachen@astro.uu.nl

(July 11, 2024)

We obtain the maximum diffuse neutrino intensity predicted by hadronic photoproduction models of active galactic nuclei, and other sources such as gamma ray bursts, that is consistent with the observed cosmic ray spectrum and diffuse extragalactic gamma ray background. For this, we compare the contributions to the cosmic ray intensity of extragalactic neutrino sources with the experimental data at energies above 10^{15} eV, employing a transport calculation of energetic protons traversing cosmic photon backgrounds. We take into account source evolution, optical depth effects in the sources, and adiabatic losses of protons in magnetic fields on scales of galaxy clusters. The strongest cosmic ray bound applies to photoproduction sources which are optically thin for the emission of neutrons, and for which adiabatic losses of the protons resulting from neutron decay can be neglected. We find that our upper bound is strongly energy dependent, and is much higher than the bound obtained by Waxman and Bahcall [1] at most energies, agreeing only at a neutrino energy of $\sim 10^{18}$ eV. As a corollary of our work we find that the present-day flux of cosmic rays from gamma ray bursts falls short of explaining the observed cosmic rays above 10^{19} eV, if the gamma ray burst luminosity density evolves similarly to that of galaxies or active galactic nuclei and if they emit equal fluxes of gamma rays and protons. We also confirm that hadronically emitting active galactic nuclei can produce both the extragalactic gamma ray background and cosmic rays at highest energies, implying interesting event rates in large underwater or deep-ice neutrino detectors.

I. INTRODUCTION

The connection between the emission of accelerated nucleons, gamma rays, and neutrinos from astrophysical sources is of considerable interest for the solution of the problem of the origin of cosmic rays [2]. If protons are accelerated in cosmic sources, their hadronic energy losses inevitably give rise to secondary gamma rays, and neutrinos via the pion decays $\pi^0 \rightarrow \gamma\gamma$ and $\pi^+ \rightarrow \mu^+ \nu_\mu \rightarrow e^+ \nu_e \nu_\mu \bar{\nu}_\mu$. Neutrinos are directly ejected due to their low interaction cross section. Gamma rays and secondary electrons, however, initiate electromagnetic cascades shifting the power from ultra-high energies to energies below which the absorption of gamma rays by pair production is unimportant. Hence it follows that the gamma ray spectrum is in general different from that of ejected cosmic rays and neutrinos. The extreme case that neither nucleons nor gamma rays escape from their sources is difficult to reconcile with the requirement of a collisionless plasma for particle acceleration. Particle acceleration does, however, require the presence of a ‘confining’ magnetic field and this may lead to adiabatic losses of the charged particles leaving the accelerator and doing expansion work against the external medium. However, neutrons produced in photo-hadronic interactions (e.g. $p\gamma \rightarrow n\pi^+$) are not magnetically confined, and can therefore be ejected without losses provided that the optical depth for reconversion into a proton $\tau_{n\gamma}$ is small which leads to very hard cosmic ray spectra. Considering all the possibilities, a robust bound for models of cosmic neutrino production based on the observed cosmic rays must be valid for a wide range of particle spectra. The recently published bound by Waxman & Bahcall [1] uses rather restrictive assumptions on the ejected cosmic ray spectra.

The discovery of a large number of powerful extragalactic gamma ray sources associated with the radio jets emerging from active galactic nuclei (AGN) [3] some of which can even be detected at TeV energies agrees with models in which protons and electrons are accelerated to ultra-high energies at shock waves and lose energy by photoproduction of pions $p\gamma \rightarrow p\pi^0$ and $p\gamma \rightarrow n\pi^+$ [4]. Collisions of the hadronically induced gamma rays with the electronic synchrotron photons $\gamma\gamma \rightarrow e^+ + e^-$ are most important for the absorption of ultra-high energy gamma rays for most parts of the jets and this leads to gamma ray spectra peaking below TeV energies [5]. The shape of the multi-TeV spectra has been correctly predicted by the hadronic model [6]. Just a small admixture of accelerated polluting baryons which remains undetected in observations sensitive to the dielectric properties of the plasma such as polarization and Faraday rotation [7] could contribute strongly to the non-thermal pressure of the extragalactic sources and supply a flux of extragalactic cosmic rays with energies up to $\sim 10^{20}$ eV, along with gamma rays and neutrinos [5]. In the expanding fireball model [8] for gamma ray bursts (GRB), the physics of the relativistic shocks is similar to

that in AGN jets, allowing us to draw some interesting parallels regarding their possible role in accelerating the highest energy cosmic rays [9,10].

Extragalactic radio sources are strongly evolving in their luminosity density, and this implies that the cascading of the gamma rays traversing intergalactic radiation fields shifts most of their gamma ray emission into the window below ~ 30 GeV [11] where EGRET on board the Compton Gamma Ray Observatory has measured an extragalactic gamma-ray background [12]. In addition to the observed cosmic ray fluxes, this gamma ray flux can be used to obtain an upper limit to the integral fluxes of extragalactic neutrinos and to exemplify the intimate connection between the hadronically induced emissions. If a sizable fraction of the extragalactic gamma ray background originates from hadronic processes, the corresponding neutrino fluxes would produce interesting event rates in large underwater/ice neutrino detectors currently planned or under construction [13].

The outline of our paper is as follows: In Sect.II we compute the ratios of cosmic ray, neutrino, and gamma ray fluxes from decay and interaction kinematics, assuming photoproduction of pions and pairs. We also quantify the effects of adiabatic losses and optical depth on these ratios. Then we proceed using the observed cosmic ray spectrum at energies down to 10^{15} eV to construct a robust upper bound for extragalactic neutrinos in Sect.III. In Sect.IV we improve the accuracy of our analytical result for the bound by employing the simulation method for cascading in the intergalactic medium developed by Protheroe & Johnson [14]. We also discuss how adiabatic losses of protons traversing magnetic fields on scales of galaxies and galaxy clusters can further relax this limit. Finally, in Sect. V we discuss various bounds and their relation with some models of extragalactic neutrino production, and discuss the observability of neutrinos from photoproduction sources in the context of these bounds.

II. COSMIC RAY, GAMMA-RAY, AND NEUTRINO EMISSION FROM EXTRAGALACTIC PROTON ACCELERATORS

A. Photo-hadronic interactions

The physics of photo-hadronic interactions can be summarized by the average values of the cross section, $\langle \sigma_{p\gamma} \rangle$, the energy loss efficiency, $\langle \kappa_p \sigma_{p\gamma} \rangle$ with $\kappa_p = \Delta E_p / E_p$ called the inelasticity of the process, and pion multiplicity and fractional energy, $\langle N_\pi \sigma_{p\gamma} \rangle$ and $\langle \sigma_{p\gamma} E_\pi / E_p \rangle$. The average over a kinematical quantity Y for interactions in a given differential background photon number density $n(\epsilon) = dN/d\epsilon dV$, with total density $n_{\text{tot}} = \int_{\epsilon_{\text{min}}}^{\infty} d\epsilon n(\epsilon)$, we define as

$$\langle Y \rangle = \sum_i \int_{\epsilon_{\text{min},i}}^{\infty} d\epsilon \frac{n(\epsilon)}{8n_{\text{tot}} \epsilon^2 E_p^2} \int_{s_{\text{min}}}^{s_{\text{max}}(\epsilon)} ds (s - m_p^2 c^4) \int_{\mathcal{F}_i} d\mathbf{f}_i Y(s, \mathbf{f}_i) \quad (1)$$

where the inner integral and the sum extend over the final states \mathcal{F}_i of all involved partial processes, and

$$s = m_p^2 c^4 + 2\epsilon E_p (1 - \beta_p \cos \theta), \quad (2)$$

is the squared center-of-momentum interaction energy for a proton of energy E_p and velocity $\beta_p c$, and a photon of energy ϵ , colliding at an angle θ in the lab-frame, $s_{\text{min},i}$ is the threshold for the process in question, $\epsilon_{\text{min},i} = (s_{\text{min},i} - m_p^2 c^4) / 4E_p$ the corresponding photon energy for $\cos \theta = -1$, and $s_{\text{max}}(\epsilon) = m_p^2 c^4 + 4\epsilon E_p$. For power law photon spectra, $n(\epsilon) \propto \epsilon^{-\alpha-1}$ (typically $\alpha = 1$ in extragalactic synchrotron sources), one finds for photopion-production $\langle \sigma_\pi \rangle \approx 100 \mu\text{barn}$, and

$$\langle \kappa_p \rangle = \langle \kappa_p \sigma_\pi \rangle / \langle \sigma_\pi \rangle \approx 0.22 \quad (3)$$

$$\langle N_\pi \rangle = \langle N_\pi \sigma_\pi \rangle / \langle \sigma_\pi \rangle \approx 1.5 \quad (4)$$

$$\langle E_\pi / E_p \rangle = \langle \sigma_\pi E_\pi / E_p \rangle / \langle \sigma_\pi \rangle \approx 0.15 , \quad (5)$$

almost independent of the power law index for $\alpha \geq 1$, and $\langle N_{\pi^\pm} \rangle \approx 2 \langle N_{\pi^0} \rangle$ [15]. We note that the average value for the cross section is lower than the actual photopion cross section as defined by Eq. (1) at most photon energies, since the definition of n_{tot} includes photons which are kinematically below the interaction threshold. The average fractional energy injected in secondary neutrinos and gamma rays per interaction for a power law photon spectrum is then given by $\xi_\nu = \frac{3}{4} \langle N_{\pi^\pm} \rangle \langle E_\pi / E_p \rangle \approx 0.11$, and $\xi_\gamma = (\frac{1}{4} \langle N_{\pi^\pm} \rangle + \langle N_{\pi^0} \rangle) \langle E_\pi / E_p \rangle \approx \xi_\nu$, respectively. Using $\langle \sigma_{p \rightarrow n} \rangle \approx \frac{1}{2} \langle \sigma_\pi \rangle$, we can define in the same way $\xi_p \approx \xi_n \approx 0.39$. Defining $\kappa_{p\nu} \simeq \kappa_{n\nu} = \langle E_\nu \rangle / \langle E_n \rangle = (1/4) \langle E_\pi / E_p \rangle / (1 - \langle \kappa_p \rangle)$ we obtain $\kappa_{n\nu}^{-1} = 20.8$. The contribution of the Bethe-Heitler process to the production of gamma-rays depends on the spectral index since its cross section peaks at energies about two orders of magnitude lower than that of photopion production. Assuming that the power law extends over this range without change, one can find the relation

$$L_\gamma = [1 + \exp(5\alpha - 5)] L_\nu , \quad (6)$$

where L_γ and L_ν are the bolometric photo-hadronic luminosities in gamma rays and neutrinos [10].

An important parameter for determining the nature of pion photoproduction sources is the optical depth of the source for $n\gamma$ interactions in which the emerging nucleon is a proton, $\tau_{n\rightarrow p}$. This is related to the photo-hadronic optical depth, $\tau_{p\gamma}$, which we can estimate from observations of AGN. We define the photo-hadronic optical depth by $\tau_{p\gamma} = t_p/t_{p\gamma}$, where $t_{p\gamma}$ is the photo-hadronic cooling time scale and t_p the mean time a proton resides in the source, $t_p^{-1} = t_{p,\text{cool}}^{-1} + t_{p,\text{ej}}^{-1}$, where $t_{p,\text{cool}}$ and $t_{p,\text{ej}}$ are total proton cooling and the direct proton ejection time scales respectively. In a freely expanding relativistic plasma (e.g., an unconfined jet or a GRB fireball), proton cooling is dominated by adiabatic losses, $t_{p,\text{cool}} \sim t_{\text{ad}} \approx R/c < t_{p,\text{ej}}$, and so $\tau_{p\gamma} \sim R/ct_{p\gamma}$, where source radius, R , and $t_{p\gamma}$ can in principle be estimated from the observed luminosity and variability time scale [10]. However, the generally unknown Doppler boosting of relativistic plasmas introduces a significant model-dependence since the Doppler factor enters with a high power in $\tau_{p\gamma}$.

Another approach is to use estimates of the $\gamma\gamma$ pair production depth, $\tau_{\gamma\gamma}$, which is related to $\tau_{p\gamma}$ by microphysical quantities. Since estimates on $\tau_{\gamma\gamma}$ are derived from the observed gamma ray emission from the source, the Doppler boosting enters in the same way as for $\tau_{p\gamma}$, so that its effect cancels in the direct comparison. For $\alpha = 1$ we then have

$$\tau_{p\gamma}(E_p) = \frac{\langle \kappa_p \sigma_{p\gamma} \rangle}{\langle \sigma_{\gamma\gamma} \rangle} \tau_{\gamma\gamma} \left(\frac{2m_e^2 E_p}{m_p m_\pi \left[1 + \frac{m_\pi}{2m_p} \right]} \right) \approx 5 \times 10^{-4} \tau_{\gamma\gamma} ([4 \times 10^{-6}] E_p) \quad (7)$$

with $\tau_{p\gamma} \propto E_p$, where we used $\langle \kappa_p \sigma_{p\gamma} \rangle \approx 30 \mu\text{barn}$ (corrected for Bethe-Heitler pair production), and $\langle \sigma_{\gamma\gamma} \rangle \approx 0.1 \sigma_T$ from averaging the total cross section for the dominating process $\gamma\gamma \rightarrow e^+e^-$ [16] over a photon spectrum with $\alpha = 1$. We note that in an homogeneous emitter the escape probability of an interacting particle propagating in straight lines is given as a function of optical depth by

$$\mathcal{P}_{\text{esc}}(\tau) \approx \frac{1 - e^{-\tau}}{\tau}; \quad (8)$$

thus, for $\tau \gg 1$ the emission is suppressed by a factor $\tau^{-1} \propto E^{-1}$, so that the energy where $\tau_{\gamma\gamma} = 1$ is observationally revealed by a steepening of the gamma-ray spectrum. For neutrons, we even expect a break of 2α , because $\tau_{p\gamma}$ enters both in the production probability of the neutron, which saturates at $\tau_{p\gamma} > 1$, and leads to a reabsorption by $n \rightarrow p$ conversions with an optical depth $\tau_{n\rightarrow p} = \tau_{p\rightarrow n} \approx 2\tau_{p\gamma}$ [17]. The corresponding neutrino spectrum also suffers a break by α due to saturation of the photo-hadronic efficiency, but since neutrinos are not reabsorbed, the ratio of ejected cosmic ray and neutrino energy goes down with $\tau_{p\gamma}^{-1}$ for $\tau_{p\gamma} \gg 1$. In Sect. 4 we will use Eqs. (7) and (8) to estimate the optical depth for neutrons in AGN jets.

We emphasize that, while the absorption of neutrons and the magnetic confinement of protons leads to an effective reduction of the total energy ejected in cosmic rays, because their energy is converted into secondary particles (neutrinos and gamma rays) during cooling, the relation of ejected neutrino and gamma-ray luminosity, Eq. (6), does not depend on the absorption properties of the source: Energetic gamma rays are not absorbed in $\gamma\gamma \rightarrow e^+e^-$, but reprocessed due to synchrotron or inverse-Compton radiation of the produced pairs, and eventually escape from the source at energies below the energy where the mean free path for pair production equals the size of the accelerator. In extragalactic jets, this energy typically lies above 10 GeV, so that they must be regarded as highly Thomson-thin. In principle, the electromagnetic energy could appear below the MeV range in Thomson-thick sources. The physical conditions in such sources would, however, be inconsistent with the requirements for particle acceleration to ultra-high energies and therefore there is no reason for believing in their existence at present.

B. Adiabatic losses

The maximum energy achievable in a long-lived Fermi-type accelerator is determined by the requirement that the scattering length be much smaller than the radius of the accelerator. Since the scattering length is generally assumed not to be shorter than the Larmor radius of the particle (Bohm diffusion), one obtains the constraint that $E_{\text{max}} \lesssim eBR$, if B is the magnetic field strength and R is the size of the accelerator. Accelerated particles with a canonical power law spectrum close to $dN/dE \propto E^{-2}$ are then advected downstream with the flow. To release the cosmic rays from the flow, the magnetic field must decrease. If this decrease is adiabatic with respect to the Larmor motion of the protons (e.g., adiabatic expansion),

$$\frac{B}{|dB/dr|} \gg r_{\text{L},p} = \frac{E_p}{eB}, \quad (9)$$

the energy of the confined protons upon their release at a lower magnetic field B_{ej} is given by

$$E_{p,\text{ej}} = E_p \sqrt{B_{\text{ej}}/B}. \quad (10)$$

We note that if $B \propto r^{-a}$ with $a \leq 2$ outside the shock regime, then Eq. (9) generally applies for particles with $E \ll E_{\max}$, since $R \lesssim R_B \equiv B/|dB/dr|$. For UHE cosmic ray accelerators discussed in the literature, magnetic field strengths at the shock range from mG in FR-II hot spots [18] to $> 10^3$ G in GRBs [10]. If the magnetic field decreases adiabatically to the typical values assumed for large scale fields (\sim nG), Eq. (10) implies energy losses of several orders of magnitude. The efficient production of observable cosmic rays extending as a power law over a considerable energy range below E_{\max} therefore requires that adiabatic losses at ejection are avoided. This can be achieved in essentially two ways: (a) the magnetic field decreases non-adiabatically from the accelerator to the large scale environment, e.g. at strong termination shocks or contact discontinuities, or (b) the proton is ejected via isospin-flip in photo-hadronic interactions as a neutron, which does not interact with the magnetic field and therefore does not suffer adiabatic losses. Process (b), on which we shall concentrate hereafter, is crucial for deriving an upper bound on the flux of extragalactic neutrinos since it has the highest neutrino (and gamma ray) yield.

III. BOUND ON THE NEUTRINO FLUX FROM THE OBSERVED COSMIC RAY FLUX

A. Energy-loss horizons

While neutrinos, as well as gamma-rays below ~ 30 GeV [11], reach us from any cosmic distance of interest, extragalactic cosmic rays suffer energy losses from photo-hadronic interactions with cosmic backgrounds, mainly the microwave background. The energy-dependent horizon for UHE cosmic ray protons, i.e., the distance over which a proton loses most of its energy, can be expressed as

$$\lambda_p(E) = c E_p / |dE_p/dt| = [n_{\text{bg}} \langle \kappa_p \sigma_{p\gamma} \rangle]^{-1}. \quad (11)$$

Photo-pion production and Bethe-Heitler pair production govern the energy loss in different energy regimes due to their very different threshold energies. The Bethe-Heitler process limits the propagation of protons with energies $E_p > 2m_p m_e c^4 / kT_{\text{mbr}} \approx 4 \times 10^{18}$ eV to $\lambda_p \sim 1$ Gpc, while pion production reduces the horizon for protons with $E_p \gtrsim m_p m_\pi c^4 / kT_{\text{mbr}} \approx 5 \times 10^{20}$ eV to $\lambda_p \sim 10$ Mpc. This is the reason for the Greisen-Zatsepin-Kuzmin (GZK) cutoff expected for a cosmic ray spectrum originating from a cosmologically homogeneous source distribution [19,20].

Another, independent, energy loss process affecting UHE protons as well as any other relativistic particle is the cosmological expansion, which involves cosmological parameters such as the Hubble constant, $H_\circ = 50h_{50} \text{ km s}^{-1} \text{ Mpc}^{-1}$ with $1 \leq h_{50} \leq 2$, the density parameter $0 < \Omega \lesssim 1$ and the cosmological constant $\Lambda \geq 0$. For the relation between distance and redshift, Ω and Λ are mainly important at large redshifts which are of minor relevance here, so we adopt for simplicity an Einstein-de Sitter cosmology with $\Lambda = 0$ and $\Omega = 1$. The horizon $\lambda_p(E_p)$ can then be related to a redshift $z_p(E_p)$ by the redshift-distance relation

$$\lambda(z) = \frac{2}{3} \frac{c}{H_\circ} \left(1 - (1+z)^{-3/2} \right) \quad (12)$$

For $E_p \approx 10^{19}$ eV, $\lambda_p \approx 1$ Gpc corresponds to $z_p \approx (0.27h_{50} - 0.06) \sim 0.2$, and only sources up to this redshift contribute to the cosmic ray spectrum at this energy. Eq. (12) can be simplified by normalizing the proton horizon to the radius of the Einstein-de Sitter universe,

$$\hat{\lambda}_p \equiv \frac{3H_\circ \lambda_p}{2c}, \quad (13)$$

which allows to write $1 + z_p = (1 - \hat{\lambda}_p)^{-2/3}$. To write $\hat{\lambda}_p$ as a function of proton energy, we decompose it as

$$\hat{\lambda}_p^{-1} = \hat{\lambda}_z^{-1} + \hat{\lambda}_{p,\text{BH}}^{-1} + \hat{\lambda}_{p,\pi}^{-1} \quad (14)$$

into the components expressing redshift, Bethe-Heitler and pion production losses, which can be written as

$$\begin{aligned} \hat{\lambda}_z &= 1 - e^{-3/2} \simeq 0.78 \\ \hat{\lambda}_{p,\text{BH}} &\approx 0.27h_{50} \exp(0.31/E_{19}) \\ \hat{\lambda}_{p,\pi} &\approx 5 \times 10^{-4} h_{50} \exp(26.7/E_{19}), \end{aligned} \quad (15)$$

where $E_{19} = E_p/10^{19}$ eV. The approximations for $\hat{\lambda}_{p,\text{BH}}$ and $\hat{\lambda}_{p,\pi}$ fit the exact functions determined numerically in [14] and the exact interaction kinematics within $\sim 10\%$ up to $E_p \sim 10^{21}$ eV. The redshift horizon $\hat{\lambda}_z$ is determined consistently with the definition of other loss processes by the redshift which reduces the energy of the particle by $1/e$, so that within the horizon $\hat{\lambda}_p$ all energy losses (including redshift) can be neglected. Obviously, the horizons for neutrinos and gamma rays below 20-30 GeV are $\hat{\lambda}_\gamma = \hat{\lambda}_\nu = \hat{\lambda}_z$.

B. Effect of the energy-loss horizons on diffuse isotropic background emissions

Galaxies and AGNs evolve similarly with cosmic time (redshift). Generally, their luminosity per co-moving volume has a pronounced peak at redshifts of $z \sim 2$, and declines or levels off at higher redshifts. A particular parametrization of the redshift-dependence of the (co-moving frame) UV luminosity density of AGNs as inferred by Boyle and Terlevich [21], assuming an Einstein-de Sitter cosmology and $h_{50} = 1$, is given by

$$\frac{\Psi_{\text{BT}}(z)}{\Psi_{\text{BT,max}}} = \begin{cases} [(1+z)/2.9]^{3.4} & : z < 1.9 \\ 1.0 & : 1.9 \leq z < 3 \\ \exp[-(z-3)/1.099] & : z \geq 3 \end{cases}, \quad (16)$$

where $\Psi_{\text{BT,max}} = (3.0 \pm 0.3) \times 10^{44} \text{ erg s}^{-1} \text{ Mpc}^{-3}$. In the next section, we will use this luminosity density function to describe the evolution of the hadronic luminosity density in the universe by simply putting

$$\Psi_{\text{had}}(z) = \frac{dL_{\text{had}}}{dV_c} = f_{\text{had}} \Psi_{\text{BT}}(z) \quad (17)$$

with some constant factor factor f_{had} . Since in the approach followed here, the integration over redshift is limited to $z \lesssim 1.7$ due to the horizon for redshift energy losses, we can use here the simplified relation $\Psi_{\text{had}} \propto (1+z)^k$ with $k = 3.4$ for the entire range of the integration.

The different energy-loss horizons for protons, gamma rays, and neutrinos, discussed in the previous section, strongly affect the relative intensities of the diffuse isotropic background fluxes from evolving source populations such as AGNs, galaxies, or GRBs (if they trace star formation activity). Cosmic rays above the ankle originate only from sources within $z_p \sim 0.2$ while neutrinos and gamma rays originate from sources within $z_\nu = z_\gamma \sim 2$. Because of the strong luminosity evolution, and because $z_\nu = z_\gamma \gg z_p$, the present-day extragalactic cosmic ray flux is strongly reduced compared with that of neutrinos and gamma rays.

The present-day spectral energy density, $u_{p,\nu}^{\circ}(E_{p,\nu}) = E_{p,\nu}^2 (dN_{p,\nu} / dE_{p,\nu} dV)$ is then given by integration over z as

$$u_{p,\nu}^{\circ}(E_{p,\nu}) = \frac{E_{p,\nu}^2}{c} \int_0^{z_{p,\nu}} \frac{\Psi_{\text{had}}(z, k) Q_{p,\nu}(E_{p,\nu})}{4\pi d_L^2(z)} \frac{dV_c(z)}{dz} dz, \quad (18)$$

where $Q_{p,\nu}(E_{p,\nu}) = dN_{p,\nu}(E_{p,\nu}) / (dE_{p,\nu} d\mathcal{L}_{\text{had}})$ is the number of injected particles at energy $E_{p,\nu}$ per unit particle energy interval per unit total injected hadronic luminosity. Again, we note that the effect of redshift energy losses is considered in the definition of the horizon (in the same way as the much stronger energy losses due to interactions with the microwave backgrounds), thus appear in the upper limit of the integral and are not explicitly considered in the integrand. In the same way, effects of the evolution of the density and temperature of the microwave background are disregarded. Inserting the Einstein-de Sitter expressions for luminosity distance, $d_L = (2c/H_0)(1+z-\sqrt{1+z})$, and differential co-moving volume, $dV_c/dz = (16\pi c^3/H_0^3)(1+z)^{-5/2}(\sqrt{1+z}-1)^2$, yields $u_{p,\nu}^{\circ} \propto (1+z_{p,\nu})^{k-5/2} - 1$, and after replacing redshift with the horizon $\hat{\lambda}_{p,\nu}$ we obtain

$$\frac{u_p^{\circ}(E_p)}{u_\nu^{\circ}(\kappa_{p\nu} E_p)} \geq \mathcal{P}_{\text{esc},n} \frac{\xi_n}{\xi_\nu} \frac{(1-\hat{\lambda}_p(E_p))^{(5-2k)/3} - 1}{(1-\hat{\lambda}_\nu)^{(5-2k)/3} - 1}. \quad (19)$$

The equality above applies if the direct emission of protons from the sources can be neglected.

The observed present day cosmic ray density $u_{\text{CR}}^{\circ} = (4\pi/c) E^2 I(E)$ can be approximated by [22]

$$\frac{E^2 I(E)}{\text{GeV cm}^{-2} \text{s}^{-1} \text{sr}^{-1}} \approx \begin{cases} 2.9 \times 10^{-8} E_{19}^{-1.07} & : \log[E_{19}] \leq 1.2 \\ 2.6 \times 10^{-8} E_{19}^{-0.70} & : \log[E_{19}] > 1.2 \end{cases}. \quad (20)$$

Using the observed cosmic ray energy density, Eq. (19) represents an energy-dependent upper bound on extragalactic neutrino fluxes, which is shown in Fig. 1 for $\mathcal{P}_{\text{esc},n} = 1$ and $h_{50} = 1$. Different choices of cosmology do not strongly affect the result, since both the derivation of the luminosity and evolution function from data and the transport of cosmic rays from large redshifts are affected in essentially the same way, so that the net effect cancels (for a discussion see Ref. [18]). Our result shown in Fig. 1 is compared with the bound derived by Waxman and Bahcall [1] and is found to agree with it only at $E \sim 10^9 \text{ GeV}$. At higher and lower energies our bound is higher by a very large factor and demonstrates in a simple way that the energy-independent bound derived by Waxman and Bahcall only applies at a neutrino energy $\sim 10^{-2}$ times the energy at which their assumed cosmic ray intensity from photoproduction sources was normalized to the highest energy cosmic ray data. The reason for the discrepancy is that Waxman & Bahcall assumed an overall extragalactic cosmic ray input spectrum of $dN/dE \propto E^{-2}$ and is therefore model dependent, while our bound removes this model dependency by comparing directly to the observed cosmic ray spectrum at all energies. Model dependency enters our bound mainly through the factor P_{esc} , and models with optically thick neutron emission could produce much higher neutrino fluxes as shown in Fig. 6. We shall improve on the limitations of the above approximations in the next section, where we also include a discussion of adiabatic losses.

IV. SIMULATION OF COSMIC RAY AND NEUTRINO SPECTRA FROM BLAZARS

The validity of the upper bound for the neutrino flux implied by the observed cosmic ray spectrum derived in the previous section suffers from various caveats and simplifications: not only does it neglect source specific properties such as optical depth and adiabatic losses in surrounding magnetic fields, it is also inaccurate in terms of the transport of extragalactic UHE protons since it does not consider the exact energy evolution of the particles, and the evolution of cosmic photon backgrounds, which have a strong effect on the contribution of high redshift sources below the ankle [23,18]. To obtain more detailed results on the relation of cosmic ray and neutrino fluxes we here employ the technique described in refs. [24,25] in which the propagation of particles and their debris is followed by a matrix method in which the matrix elements are calculated by Monte-Carlo simulation using exact cross sections where available. This, and the assessment of the effects of adiabatic losses requires us to adopt an assumption about the source population. We restrict ourselves to radio-loud AGN, since they are expected to be bolometrically most important in the high-energy Universe. However, we shall demonstrate that our results are rather insensitive to this assumption.

In the Monte-Carlo/matrix method [14] fixed logarithmic energy bins were used, and the energy spectra of particles of type $\alpha, \beta = \gamma, e, p, n, \nu_e, \bar{\nu}_e, \nu_\mu, \bar{\nu}_\mu$ at distance x in the cascade are represented by vectors $F_j^\alpha(x)$ which give the total number of particles of type α in the j th energy bin at distance x . Transfer matrices, $T_{ij}^{\alpha\beta}(\delta x)$, give the number of particles of type β in bin j which result from propagation through a thin slab of thickness δx after a particle of type α and energy in bin i initiates a cascade. Then, given the spectra of particles at distance x one can obtain the spectra at distance $(x + \delta x)$

$$F_j^\beta(x + \delta x) = \sum_{\alpha} \sum_i T_{ij}^{\alpha\beta}(\delta x) F_i^\alpha(x) \quad (21)$$

where $F_i^\alpha(x)$ are the spectra (number in the i th energy bin) of species α at distance x . The transfer matrices depend on particle yields, $Y_{ij}^{\alpha\beta}$, which are defined as the probability of producing a particle of type β in the energy bin j when a primary particle of type α with energy in bin i undergoes an interaction. To calculate $Y_{ij}^{\alpha\beta}$ a Monte Carlo simulation was used [14].

We could also write the equations for propagation through a thin slab as

$$[F(x + \delta x)] = [T(\delta x)][F(x)] \quad (22)$$

where the matrix $[T]$ is now a matrix containing all the transfer matrices $T_{ij}^{\alpha\beta}$, and the vector $[F]$ contains all the vectors F_i^α . Once the transfer matrices have been calculated for propagation through a distance δx , the transfer matrix for propagation through a distance $n\delta x$ is simply given by applying the transfer matrices n times, i.e.

$$[T(n\delta x)] = [T(\delta x)]^n. \quad (23)$$

In this way, cascades over long distances can be modeled quickly and efficiently. A small complication is introduced by the cosmological redshift, which changes also the temperature and density of the background fields, i.e. $T(z) = (1+z)T_0$ and $n_\gamma(z) = (1+z)^3 n_\gamma^0$. To account for this, matrices have to be recalculated as soon the change of energy due to redshift approaches the bin size, i.e. $\log(1+z) = 0.1$. The technical details of the matrix-method, the computation of the transfer matrices and the application to extragalactic proton and photon transport has been described in detail by Protheroe & Johnson [14].

In the present problem, we consider an injection spectrum of $Q_\alpha(E, z) = Q_\alpha(E)\Psi_{\text{had}}(z)dV_c/dz$ particles of type $\alpha = p, \nu_\mu, \bar{\nu}_\mu$ per unit redshift per unit energy per unit time where $\Psi_{\text{had}}(z)$ is the power per co-moving volume injected in particles escaping from AGN or similarly evolving source populations. Then the intensity at Earth at energy E is obtained by integrating over redshift (up to $z = 10$) the contributions to the flux taking account of the necessary cosmological factors. Thus we include the exact energy evolution of the cosmic ray nucleon and neutrino spectra during transport, which was disregarded in Eq. (18).

To estimate the cosmic ray ejection spectrum from blazar jets, $Q_{p+n}(E)$, we need to discuss (a) possible mechanisms for direct ejection of protons from the magnetic field of the jet, and (b) the photo-hadronic optical depth relevant for the production and absorption of neutrons. Starting with (b), we can use the observed break at ~ 0.4 TeV in the gamma-ray spectrum of Mrk 501 [26] which, in the hadronic models, is naturally explained as due to absorption by $\gamma\gamma$ pair production [5], i.e. $\tau_{\gamma\gamma}(0.4 \text{ TeV}) \approx 1$. From Eq. (7) we then find that $\tau_{p\gamma} \approx 0.04 E_{19}$. Mrk 501 is a low-luminosity blazar, and since $\tau_{p\gamma} \propto L_0$ is expected (suppressing here the other dependences on the size of the accelerator and the bulk Lorentz factor), the photo-hadronic optical depth may reach unity for blazars with $L_0 \gg L_{\text{Mrk 501}}^{\text{Mrk 501}} \sim 3 \times 10^{44} \text{ erg s}^{-1}$ for $E_p \lesssim 10^{19} \text{ eV}$. However, averaging over the luminosity function of blazars given by Wolter et al. [27], $dN/dL_0 \propto L^{-1.6}$ in the range $3 \times 10^{43} - 10^{46} \text{ erg s}^{-1}$ gives $\langle \tau_{p\gamma} \rangle_{\text{bl}} \approx 0.05 E_{19}$, thus only a small correction to the result for Mrk 501. Using the average as a canonical value and considering $\tau_{n \rightarrow p} \approx 2\tau_{p\gamma}$, this shows that there is at least a subclass of all AGN jets (the low-luminosity blazars) which can be regarded as optically thin for neutrons up to $E_n \sim 10^{20} \text{ eV}$, and the ejected neutron spectrum would then be $\propto E^{-1}$ without a break up to $E \leq E_{\text{max}} \lesssim eBR$.

Concerning (a), we note that the flow of the jet keeps the advected protons of all energies $E_p < E_{\max} \lesssim eBR$, including the accelerated protons, confined in the jet magnetic field, such as $B \propto R^{-1}$ characteristic of a free jet. Since at the acceleration site $B \sim 30$ G in hadronic AGN models, adiabatic expansion down to typical galaxy halo field strengths $B \lesssim 1$ μ G leads to adiabatic losses of 3–4 orders of magnitude. Therefore, direct ejection of VHE-UHE protons is only possible by diffusion sideways across the boundary of the jet. However, the acceleration region in hadronic jet models is located at distances of ~ 0.01 – 0.1 pc from the central Black Hole, well inside the broad line region (BLR) of the AGN for which the equipartition argument leads to estimated magnetic field strengths of ~ 1 G. If this BLR field decays adiabatically over a scale $R_B \sim 0.1$ pc, the adiabatic energy loss of the confined protons would be comparable to the case of the protons advected out along the jet. In addition, the isotropisation of the proton distribution function, owing to gyration in the BLR field, would make them subject to photo-hadronic interactions with the UV-photons from the AGN accretion disk. Assuming a random walk of the protons, and disregarding adiabatic losses for the moment, this leads to optical depths of $\tau_{p\gamma} \gg eBL_{\text{UV}}\sigma_{p\gamma}/4\pi ckT_{\text{UV}}E_p \approx B_{\text{GL45}}E_{19}^{-1}$, thus $\tau_{p\gamma} \gg 1$ in the canonical case. Hence, protons directly ejected from the jet cannot escape the BLR of the AGN; they would either lose energy adiabatically, or in photo-hadronic interactions with the UV field. In the latter case, they produce neutrons and neutrinos, directed typically towards the accretion disk from where the radiation emerges because head-on collisions are kinematically favored. Thus, the neutrons produced in this way are likely to be reabsorbed in subsequent interactions with the strong radiation field and high matter density in the accretion disk, while the neutrinos can cross the disk and escape. The BLR would therefore contribute as an optically thick photo-hadronic emitter to the neutrino flux, but not to the cosmic ray flux. For simplicity, we disregard this possibility hereafter and assume that the energy of these protons is lost adiabatically.

In contrast, neutrons from the jet leave the BLR before undergoing β -decay for $E_n > 10^{14}$ eV, and since they are beamed away from the accretion disk they would not strongly interact with the radiation field. Thus, if protons are accelerated with an E^{-2} differential spectrum, the photoproduced neutrons can be assumed to leave the AGN, and to be ejected with the spectrum

$$Q_n(E) = q_n(E/E_{\max})^{-1} \exp(-E/E_{\max}), \quad (24)$$

where q_n and E_{\max} are kept as free parameters. The neutron spectrum is associated with a muon-neutrino spectrum

$$Q_{\nu_\mu}(E) = \frac{2 \langle N_{\pi^\pm} \rangle \langle E_n \rangle}{\langle N_n \rangle \langle E_\nu \rangle} Q_n([\langle E_n \rangle / \langle E_\nu \rangle]E) = 83.2 Q_n(20.8E) \quad (25)$$

where we count ν_μ and $\bar{\nu}_\mu$ together, and the corresponding spectrum of electron neutrinos at the source would be $Q_{\nu_e}(E) \approx \frac{1}{2} Q_{\nu_\mu}(E)$. The spectra are very hard, such that the energy flux from a single source peaks at the highest energy. Superimposing the emissions from a large population of sources with varying maximum energies may lead to cumulative spectra very different from the single-source injection spectrum, the envelope of which is our bound discussed in the last section.

If AGN were isolated in extragalactic space, the cosmic ray injection spectrum would be $Q_{\text{cr}}(E) \approx Q_n(E)$. However, AGN are probably embedded in strong radio galaxies [28]. These are known to have radio halos (lobes) extending out to at least 10–100 kpc, and with magnetic fields $B \sim 10$ μ G. A clear edge of these lobes is not seen, so we will follow the assumption that the magnetic field drops for $R < 1$ Mpc with $B = B_0(R/R_0)^{-1}$ with $B_0 = 10$ μ G and $R_0 = 10$ kpc. At $R = 1$ Mpc, the field has then declined to a value $B_x = 0.1$ μ G, and either remains constant for larger R if supercluster magnetic fields of this strength are present, or drops non-adiabatically to lower values at a termination shock of the halo. In this case, most neutrons with $E_n < 10^{20}$ eV undergo β -decay inside the halo, and the resulting protons suffer adiabatic losses such that

$$\frac{E_{p,\text{ej}}}{E_n} = \left(\frac{B_x \lambda_{n,\beta}}{B_0 R_0} \right)^{1/2} \approx 0.3 E_{19}^{1/2} \quad (26)$$

where $\lambda_{n,\beta} \approx [100 \text{ kpc}] E_{19}$ is the β -decay mean free path of the neutron and $E_{19} = E_n/10^{19}$ eV, leading to a cosmic ray ejection spectrum

$$Q_{\text{cr}}(E) = (2/3)(10^{20} \text{ eV}/E)^{1/3} Q_n \left([E^2 10^{20} \text{ eV}]^{1/3} \right) \quad (27)$$

for $E < 10^{20}$ eV, and $Q_{\text{cr}}(E) = Q_n(E)$ for $E > 10^{20}$ eV. Certainly, the assumptions on the halo size and magnetic field strength are somewhat extreme, but not unrealistic, and we note that if most or all AGN reside in giant elliptical galaxies, it is to be expected that many of them also reside in the center of dense clusters of galaxies (as in the case of, e.g., Hydra A) giving rise to magnetic fields and decay scales which could be even larger than assumed here. In the following, we will use both Eq. (27) for the emission of cosmic rays through radio halos, and Eq. (24) for the neutron ejection from isolated AGN, to bracket the possible range of cosmic ray fluxes correlated to a given neutrino spectrum.

V. RESULTS AND DISCUSSION

Using the Monte-Carlo based matrix simulation method described in the previous section, we have injected spectra of protons (from neutron decay) and neutrinos as given by Eqs. (25) and (26) at various redshifts and propagated the spectra to Earth. This was done for 18 E_{\max} values at half-decade intervals ranging from 3×10^5 – 10^{14} GeV. The spectra resulting from the hadronic luminosity function given by Eq. (17) are then obtained by numerical integration. These propagated spectra are then normalized (i) such that the proton spectrum does not exceed the observed cosmic ray intensity as given by Eq. (20), and (ii) such that the total neutrino energy flux (all flavors) does not exceed 0.5 times the observed power-law component of the diffuse gamma-ray background (we estimate the background between 3 MeV and 30 GeV to be $\sim 1.5 \times 10^{-5}$ GeV cm^{-2} s^{-1} sr^{-1}) [12]. The maximum for each of the 18 neutrino energy spectra (i.e. maximum of $E_\nu^2 dI_\nu/dE_\nu$) is indicated by a filled circle in Fig. 2. Connecting these points we would obtain the locus of the maxima of the highest allowed neutrino energy spectra, and we shall refer to this as the “upper bound”. Strictly speaking, the neutrino energy spectrum can exceed this bound away from the energy corresponding to the maximum value of $E_\nu^2 dI_\nu/dE_\nu$, provided of course $E_\nu^2 dI_\nu/dE_\nu$ does not exceed the bound at maximum. We also show in Fig. 2 examples of propagated proton intensities and neutrino intensities which just satisfy the bound. Condition (ii) was applied to $E_{\max} = 10^7$ GeV, and to $E_{\max} = 3 \times 10^{13}$ GeV, while condition (i) was applied to $E_{\max} = 10^{10}$ GeV.

For the purpose only of comparison with the analytic bound shown in Fig. 1, we have calculated the bound using only condition (i). The results for this case are plotted as the filled circles in Fig. 1, and are found to be in excellent agreement with the analytic result below 10⁷ GeV, and within a factor of 2 up to 10⁹ GeV. We can understand the disagreement at higher energies, which arises for a number of reasons, the most important being that the analytic approximation (Eq. 20) treats all interactions as continuous energy loss processes and ignores the non-continuous nature of pion photoproduction interactions. In addition, the Monte-Carlo based matrix simulation includes the neutrino flux produced by photoproduction interactions during propagation and also includes interactions with the radio background, and so we should not expect good agreement with the analytic result at high energies. However, the analytic bound is a simple, and therefore useful, demonstration of why the bound depends on energy, a conclusion very different from that of Waxman and Bahcall.

In Fig. 3(a) we show the upper bound obtained in the same way for the case of neutrino spectra as given by Eq. (26), but proton spectra given by Eq. (28) as appropriate to protons from neutron decay losing energy by adiabatic losses. This is compared with the previous case (no adiabatic losses) and, as expected, is found to differ only for $E_\nu < 10^9$ GeV (adiabatic losses according to Eq. 28 do not affect protons with energy above 10¹¹ GeV). Nevertheless, the upper bound is significantly higher below $E_\nu < 10^9$ GeV than for the case of no adiabatic losses and the associated proton spectra are consistent with the proton component of the cosmic ray flux between 3 \times 10⁸ GeV and 10¹⁰ GeV as used in ref. [29]. This is shown more clearly in Fig. 3(b) where the spectra have been multiplied by $E^{2.75}$.

It is instructive to consider a composite neutrino spectrum arising from the superposition of many AGN with different E_{\max} values. For illustration, we have constructed such a superposition of input spectra described by Eqs. (25) and (26), i.e. with no adiabatic losses, with each component having a different E_{\max} value in the range 10⁷–3 \times 10¹⁰ GeV with a normalization chosen such that the overall proton spectrum does not exceed the observed cosmic ray spectrum, and such that the total neutrino energy flux does not exceed 0.5 times the observed diffuse gamma ray energy flux. This result is shown in Fig. 5 where individual components of the proton spectrum corresponding to each E_{\max} value are shown, as well as the total proton and total $\nu_\mu + \bar{\nu}_\mu$ spectrum.

For identical neutron and neutrino input spectra, we show the effect of the adiabatic losses on the proton spectrum in Fig. 4(a). As can be seen, while the propagated neutrino intensity remains unchanged (apart from a very slight difference due to the different contributions from neutrinos produced during propagation resulting from different cosmic ray input spectra), the proton spectrum is considerably reduced below the observed cosmic ray spectrum, and even below the estimated proton component (see Fig. 5b where the spectra are multiplied by $E^{2.75}$).

In Fig. 6 we compare the upper bounds for $\nu_\mu + \bar{\nu}_\mu$ in the present work for pion photoproduction neutrino sources for $\tau_{n\gamma} \sim 1$ with protons from neutron decay escaping freely into intergalactic space and the case where escaping protons suffer adiabatic losses as described by Eq. (28). For completeness, one should consider the somewhat unrealistic case of optically thick photoproduction sources such that no neutrons escape, either because $\tau_{n\gamma} \gg 1$, or for some other reason. Assuming the neutrino spectra are still given by Eq. (26) one would arrive at the bound labeled $\tau_{n\gamma} \gg 1$ which is shown in Fig. 6. The upper bound estimated by Waxman and Bahcall is shown for comparison, together with neutrino intensities from AGN (Mannheim model A) and GRB (Waxman and Bahcall), and an observational upper limit from Fréjus [31]. The atmospheric background [30] is shown by the hatched band since it depends on direction, being highest in the horizontal direction and lowest in the vertical direction.

An important case of young AGN jets terminating in the interstellar medium of the host galaxy may give rise to acceleration of an E^{-2} spectrum of protons which would interact in the dense shocked interstellar medium. In such pp beam dump sources, if the density is sufficiently high one may have $\tau_{np} \gg 1$. In this case only neutrinos would emerge, and their spectrum would also be $\sim E^{-2}$. Assuming an E^{-2} power-law over 10 decades in energy, and a normalization such that the neutrino energy flux does not exceed half of the observed power-law component of the diffuse X-ray to gamma-ray background we arrive at the

bound labeled $\tau_{pp} \gg 1$ as shown in Fig. 6. In Fig. 7 we also show predicted neutrino intensities from AGN [13] (model A¹) and GRBs [9].

Inspection of Fig. 6 immediately shows that GRBs emitting neutrinos, gamma rays and protons with equal fluxes (as assumed in ref. [9]) cannot explain the present-day cosmic rays above the ankle, if GRBs evolve similarly to AGNs or galaxies. Owing to evolution, most of the present-day neutrino and gamma-ray flux originates from sources at high redshifts, from which the proton flux is reduced by almost an order of magnitude compared with that of neutrinos and gamma rays due to the energy losses traversing cosmic background photon fields. Increasing the cosmic ray fraction emitted from GRBs as suggested in ref. [17] would be accompanied by higher neutrino fluxes which can be tested using future neutrino telescopes.

To illustrate how the $(\nu_\mu + \bar{\nu}_\mu)$ signals expected from different astrophysical neutrino spectra would be detected by telescopes with different energy thresholds, we have made approximate estimates of the event rates as a function of minimum muon energy using the $P_{\nu \rightarrow \mu}(E_\nu, E_\mu^{\min})$ function given in Fig. 2 of ref. [32] for $E_\mu^{\min} = 1$ GeV, modified for other E_μ^{\min} values in a way consistent with that given for $E_\mu^{\min} = 1$ TeV. The effects of shadowing for vertically upward-going neutrinos have been included using the shadow factor $S(E_\nu)$ given in Fig. 20 of ref. [33]. We have estimated the expected (non-oscillating) neutrino induced muon signal for the horizontal and vertical directions corresponding to neutrino intensities for the AGN and GRB models, and for intensities identical to the bounds shown in Fig. 6. The results are shown in Fig. 7 (a) and (b) for the horizontal and vertical directions respectively. In the case of the vertical muon intensity and muon background the effect of shadowing is included. Note that $\nu_\mu \rightarrow \nu_\tau$ neutrino oscillations would significantly change the shadowing effect, e.g. tau neutrinos of ultra-high energy will cascade in energy down to ~ 100 TeV rather than be absorbed by the Earth [34]. Hence tau neutrinos at ~ 100 TeV would be a generic feature associated with extragalactic sources of very energetic muon neutrinos.

In conclusion, we obtain a bound for diffuse neutrino fluxes from optically thin photoproduction sources which takes account of the observed luminosity evolution of AGN, and propagation through the microwave and other background radiation fields. The bound is only very weakly model-dependent (e.g. see Figs. 4 and 3a for allowed neutrino spectra resulting from very different input neutron spectra). In the important energy range below 2×10^6 GeV, we find that the relevant upper limit is given by comparison with the diffuse gamma ray background rather than with the cosmic ray spectrum. This does not imply significant changes to the normalization of current models of extragalactic neutrino sources, and is about a factor of 50 above the energy-independent bound recently claimed by Waxman & Bahcall, which we confirm only for a neutrino energy of $\sim 10^9$ GeV. At this energy, we also find only a weak influence of adiabatic losses due to magnetic fields in the environment of the sources (e.g., giant radio halos around radio loud AGN). At lower energies, however, we find that the relation between neutrino and cosmic ray fluxes is strongly affected by magnetic fields; therefore, neutrino fluxes in excess of the Waxmann & Bahcall bound are allowed even if the cosmic ray flux below $\sim 10^{10}$ GeV is dominated by galactic sources, as suggested by the tentative data on a possible composition change in the cosmic ray spectrum below this energy. Also at neutrino energies above 10^{10} GeV, the apparent absence of the Greisen-Zatsepin-Kuzmin cutoff in the cosmic ray data does not allow to apply significant limits on the neutrino flux, and again the upper limit is given by comparison with the diffuse gamma ray background. Consequently, we find that the hadronic production of the diffuse gamma ray background is not in conflict with observed cosmic ray fluxes.

[1] E. Waxman, J. Bahcall, Phys. Rev. D, accepted for publication (1999).
[2] V.S. Berezinskii, S.V. Bulanov, V.A. Dogiel, V.L. Ginzburg (ed.), V.S. Ptuskin, *Astrophysics of Cosmic Rays*, North-Holland (1990).
[3] R. Muhkerjee, *et al.*, Astrophys. J. **490**, 116 (1997).
[4] P.L. Biermann, P.A. Strittmatter, Astrophys. J. **322** 643 (1987).
[5] K. Mannheim, W. M. Krülls, and P. L. Biermann, Astron. Astrophys. **251**, 723 (1991); K. Mannheim, P.L. Biermann, Astron. Astrophys. **253**, L21 (1992); K. Mannheim, Astron. Astrophys. **269**, 67 (1993).
[6] K. Mannheim, Science **279**, 684 (1998).
[7] J.F.C. Wardle, *et al.*, Nature **395**, 457 (1998).
[8] P. Meszárós, M.J. Rees, Astrophys. J. **405**, 278.
[9] E. Waxman, J. Bahcall, Phys. Rev. Lett. **78**, 2292 (1997).
[10] J. Rachen and P. Mészáros, Phys. Rev. D **58**, 123005 (1998).
[11] P. Madau, E.S. Phinney, Astrophys. J. **456**, 124 (1996).

¹ Note that the original paper [13] also discusses model B, with its gamma ray flux saturating a spurious Apollo measurement of the MeV gamma ray background, and excludes it because of its overproduction of cosmic rays.

[12] P. Sreekumar, F. W. Stecker, and S. C. Kappadath, in *AIP Conf. Proc. 410: Proceedings of the Fourth Compton Symposium* (eds. Ch.D. Dermer, M.S. Strickman, and J.D. Kurfess, Williamsburg, VA April 1997), p. 344 (1997).

[13] K. Mannheim, *Astropart. Phys.* **3**, 295 (1995).

[14] R. J. Protheroe and P. A. Johnson, *Astropart. Phys.* **4**, 253 (1996).

[15] J. P. Rachen, Ph.D. thesis, Universität Bonn, Germany, 1996, <http://www.astro.psu.edu/users/jorg/PhD>.

[16] J. Jauch and F. Rohrlich, *The Theory of Electrons and Photons*, 2nd ed. (Springer-Verlag, New York, 1976).

[17] J. P. Rachen and P. Mészáros, in *Gamma-Ray Bursts, Procs. 4th Huntsville Symposium, Sep 15–20, 1997*, No. 428 in *AIP Conference Procs.*, edited by C. A. Meegan, R. Preece, and T. Koshut. (American Institute of Physics, New York, 1998), pp. 776–780.

[18] J. P. Rachen and P. L. Biermann, *Astron. Astrophys.* **272**, 161 (1993).

[19] K. Greisen, *Phys. Rev. Lett.* **16**, 748 (1966).

[20] G. Zatsepin and V. Kuzmin, *JETP Lett.* **4**, 78 (1966).

[21] B. J. Boyle and R. J. Terlevich, *Mon. Not. R. Astron. Soc.* **293**, L49 (1998).

[22] D. J. Bird *et al.*, *Astrophys. J.* **424**, 491 (1994).

[23] V. Berezinsky and S. Grigor'eva, *Astron. Astrophys.* **199**, 1 (1988).

[24] R.J. Protheroe, *Mon. Not. R. Astron. Soc.* **221**, 769 (1986).

[25] R.J. Protheroe, T. Stanev, *Mon. Not. R. Astron. Soc.* **264**, 191 (1993).

[26] F.W. Samuelson, S.D. Biller, I.H. Bond, *et al.*, *Astrophys. J.* **501**, L17 (1998).

[27] A. Wolter, *et al.*, *apj* **433**, 29 (1994).

[28] C. M. Urry and P. Padovani, *Publ. Astron. Soc. Pac.* **107**, 803 (1995).

[29] J.P. Rachen, T. Stanev, P.L. Biermann, *Astron. Astrophys.* **273**, 377 (1993).

[30] P. Lipari, *Astropart. Phys.* **1**, 195 (1993).

[31] W. Rhode, *et al.*, *Astropart. Phys.* **4**, 217 (1996).

[32] T. Gaisser, F. Halzen, and T. Stanev, *Phys. Rep.* **258**, 173 (1995).

[33] R. Gandhi, C. Quigg, M. H. Reno, and I. Sarcevic, *Astropart. Phys.* **5**, 81 (1996).

[34] F. Halzen, D. Saltzberg, *Phys. Rev. Lett.* **81**, 4305 (1998).

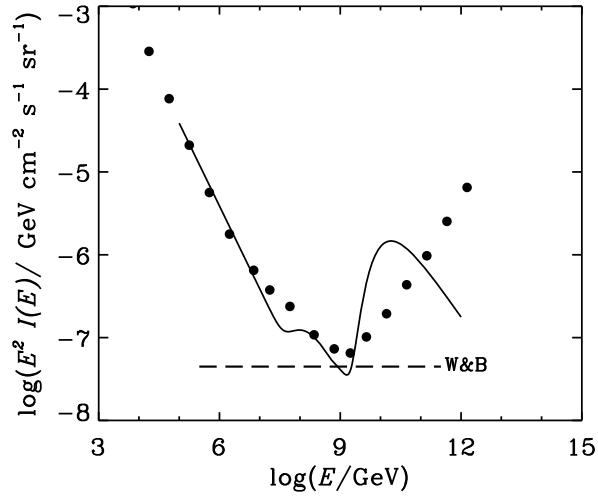


FIG. 1. Analytic result for maximum intensity of neutrinos from cosmological photoproduction neutrino sources estimated using Eq. (20) for cosmological source evolution exponent $k = 3.4$ (solid curve). The filled circles show numerical results from cascade simulations discussed in the next section for source evolution given by Eq. (16) for the case where the neutrino bound is derived assuming only that the observed cosmic ray intensity must not be exceeded. The dashed line shows the bound obtained by Waxman and Bahcall.

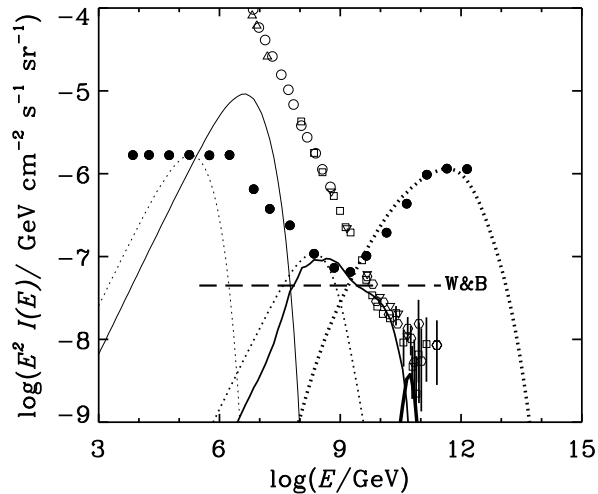


FIG. 2. Upper bound for $\nu_\mu + \bar{\nu}_\mu$ in the present work for pion photoproduction neutrino sources for the case $\tau_{n\gamma} \sim 1$ with protons from neutron decay escaping freely into intergalactic space (filled circles). Examples are given of propagated proton intensities (solid curves) and neutrino intensities (dotted curves) for $E_{\max} = 10^7$ GeV, $E_{\max} = 10^{10}$ GeV and $E_{\max} = 3 \times 10^{13}$ GeV.

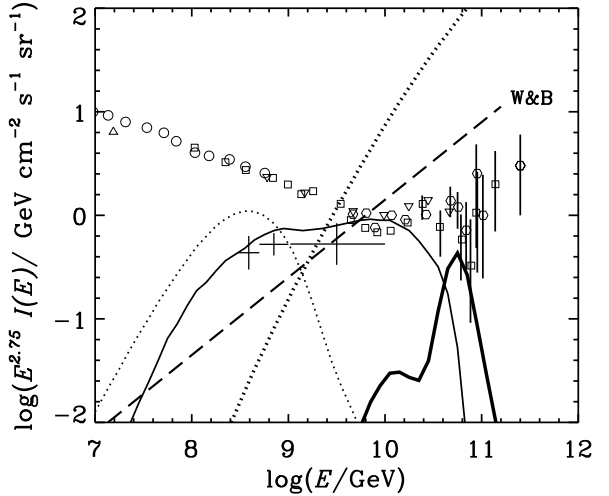
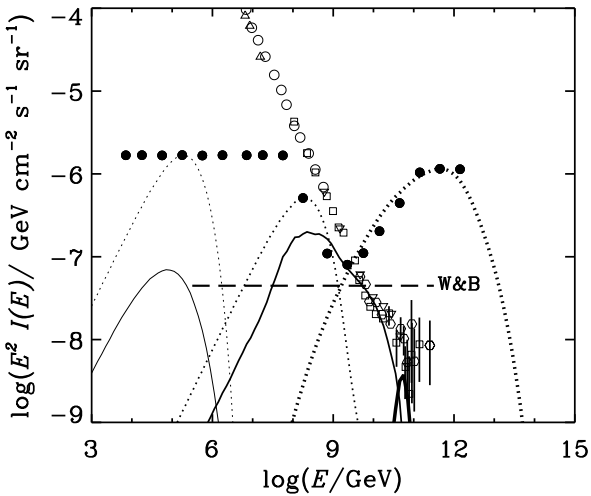


FIG. 3. (a) Upper bounds for $\nu_\mu + \bar{\nu}_\mu$ in the present work for pion photoproduction neutrino sources for $\tau_{n\gamma} \sim 1$ and with protons from neutron decay suffering adiabatic losses as described by Eq. (27). See Fig. 2 for key to curves. (b) Particle spectra from part (a) plotted multiplied by $E^{2.75}$ and compared with the observed cosmic ray spectrum, and with an estimate from Fly's Eye data of the proton component of the cosmic ray flux between 3×10^8 GeV and 10^{10} GeV (crosses).

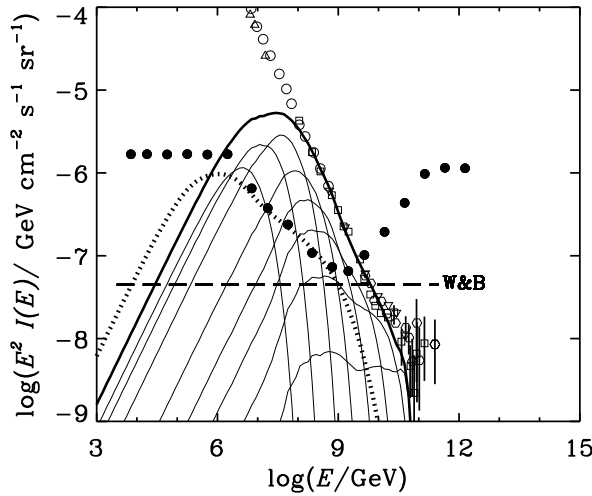


FIG. 4. Proton spectrum (thick solid line) and $(\nu_\mu + \bar{\nu}_\mu)$ spectrum (dotted curve) due to a superposition of pion photoproduction neutrino sources with protons from neutron decay escaping freely into intergalactic space. The superposition consists of input spectra described by Eq. (25) and (26) but having different E_{\max} values in the range 10^7 — 3×10^{10} GeV with normalizations chosen such that the total proton spectrum does not exceed the observed cosmic ray spectrum and the total neutrino energy flux does not exceed 0.5 times the observed diffuse gamma ray energy flux. Individual components of the proton spectrum corresponding to each E_{\max} value are also shown (thin solid curves).

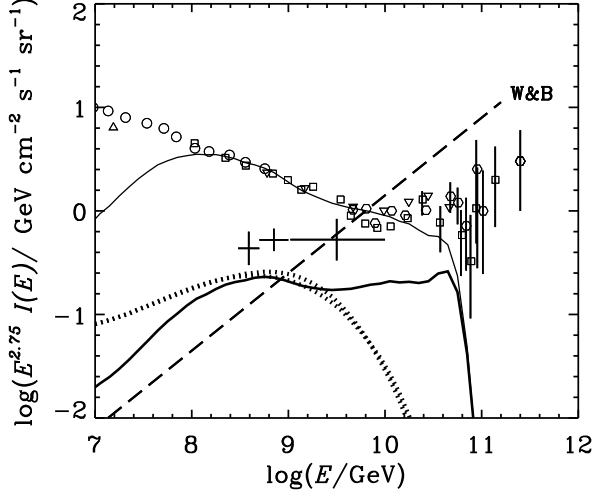
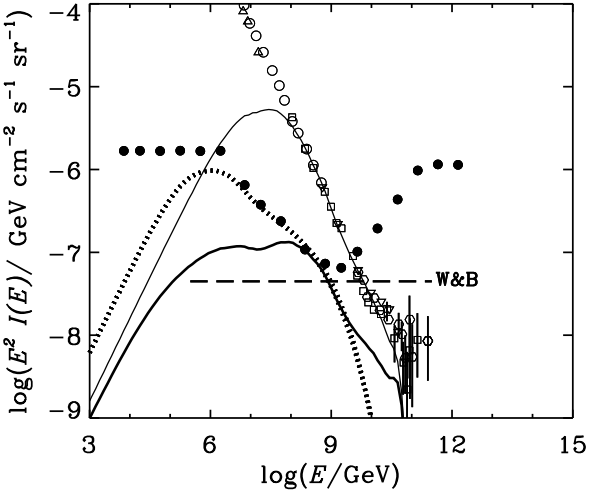


FIG. 5. (a) Proton spectrum (thin solid curve) and $(\nu_\mu + \bar{\nu}_\mu)$ spectrum (dotted curve) for the case of no adiabatic losses are identical to the spectra in Fig. 4. The thick solid curve shows how the proton spectrum is modified due to adiabatic losses (Eq. 27) for the same input neutron and neutrino spectra as in Fig. 4. (b) Particle spectra from part (a) plotted multiplied by $E^{2.75}$ and compared with the observed cosmic ray spectrum, and an estimate from Fly's Eye data of the proton component of the cosmic ray flux between 3×10^8 GeV and 10^{10} GeV (crosses).

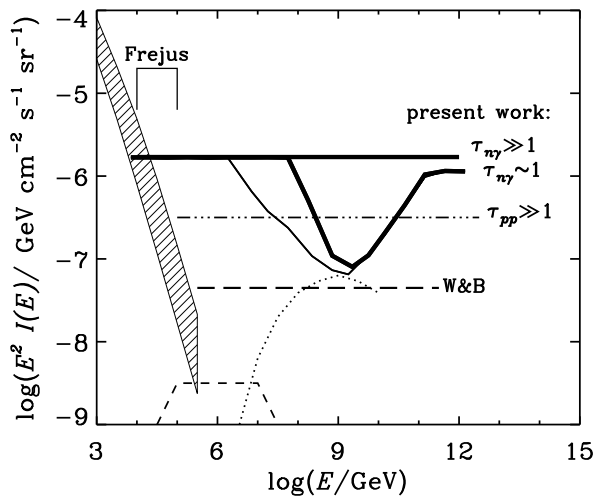
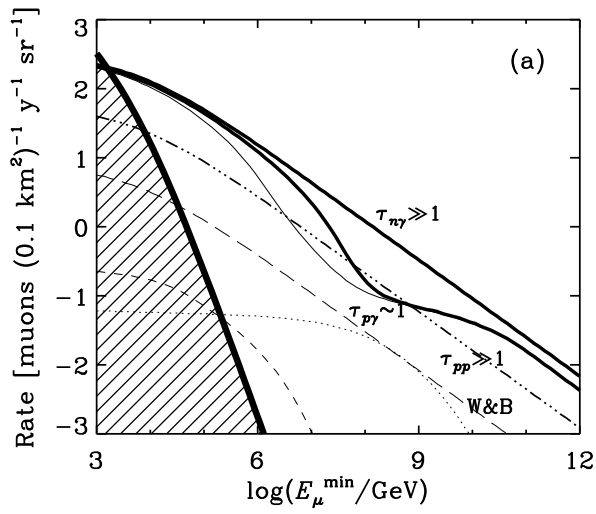
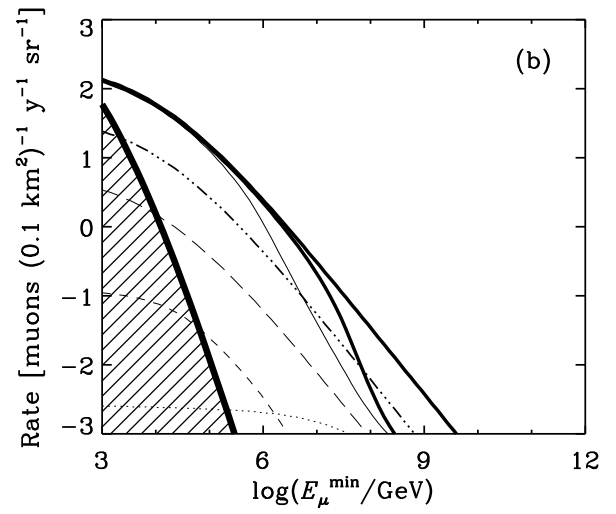


FIG. 6. Upper bounds for $\nu_\mu + \bar{\nu}_\mu$ in the present work for pion photoproduction neutrino sources (thin solid curve; curve obtained by connecting points from Fig. 2), or suffering adiabatic losses as described by Eq. (29) (thick solid curve labeled $\tau_{n\gamma} \sim 1$). Also shown are upper bounds for photoproduction neutrino sources for $\tau_{n\gamma} \gg 1$ (thick solid line labeled $\tau_{n\gamma} \gg 1$), and for the optically thick pp beam dump source case $\tau_{pp} \gg 1$ (i.e. no neutron escape, E^{-2} spectrum of neutrinos) (thick dot-dash line labeled $\tau_{pp} \gg 1$). The upper bound estimated by Waxman and Bahcall is indicated by the long dashed line labeled W&B. Neutrino intensities from AGN (Mannheim model A) and GRB (Waxman and Bahcall) are shown by the dotted curve and short dashed curve respectively. Also shown is an observational upper limit from Fréjus [31] and the atmospheric background [30].



(a)



(b)

FIG. 7. (a) Muon signal in (a) the horizontal direction, and (b) the vertical direction, resulting from neutrino intensities predicted from GRB, AGN, and from neutrino intensities identical to the bounds shown in Fig. 6. The hatched region indicated the atmospheric background signal.